Cancer Research

Arsenic Trioxide Treatment Decreases the Oxygen Consumption Rate of Tumor Cells and Radiosensitizes Solid Tumors

Caroline Diepart[1], Oussama Karroum[1], Julie Magat[1], Olivier Feron[2], Julien Verrax[2], Pedro Buc Calderon[2], Vincent Grégoire[4], Philippe Leveque[1], Julie Stockis[5], Nicolas Dauguet[5], Bénédicte F. Jordan[1], and Bernard Gallez[1]

Abstract

Arsenic trioxide (As_2O_3) is an effective therapeutic against acute promyelocytic leukemia and certain solid tumors. Because As_2O_3 inhibits mitochondrial respiration in leukemia cells, we hypothesized that As_2O_3 might enhance the radiosensitivity of solid tumors by increasing tumor oxygenation [partial pressure of oxygen (pO_2)] via a decrease in oxygen consumption. Two murine models of radioresistant hypoxic cancer were used to study the effects of As_2O_3. We measured pO_2 and the oxygen consumption rate *in vivo* by electron paramagnetic resonance oximetry and ^{19}fluorine-MRI relaxometry. Tumor perfusion was assessed by Patent blue staining. In both models, As_2O_3 inhibited mitochondrial respiration, leading to a rapid increase in pO_2. The decrease in oxygen consumption could be explained by an observed decrease in glutathione in As_2O_3-treated cells, as this could increase intracellular reactive oxygen species that can disrupt mitochondrial membrane potential. When tumors were irradiated during periods of As_2O_3-induced augmented oxygenation, radiosensitivity increased by 2.2-fold compared with control mice. Notably, this effect was abolished when temporarily clamped tumors were irradiated. Together, our findings show that As_2O_3 acutely increases oxygen consumption and radiosensitizes tumors, providing a new rationale for clinical investigations of As_2O_3 in irradiation protocols to treat solid tumors. *Cancer Res; 72(2); 482–90. ©2011 AACR.*

Introduction

The partial pressure of oxygen (pO_2) is a crucial factor in the response of tumors to irradiation and other cytotoxic treatments. Several studies have shown superior outcomes for cancer patients whose tumors had lower hypoxic fractions (1). Tumor hypoxia results from an imbalance between oxygen delivery and oxygen consumption, either of which may potentially be targeted by therapeutic interventions to transiently alleviate tumor hypoxia and potentiate cytotoxic treatments. It has been suggested that modifying oxygen consumption is more efficient at alleviating hypoxia than modifying oxygen delivery (2). Several pharmacologic drugs that inhibit cellular oxygen consumption have been characterized for their potential to increase tumor oxygenation and thereby enhance radiosensitivity. Meta-iodobenzylguanidine (3), insulin (4), anti-inflammatory drugs (5), corticoids (6), some antagonists of VEGF receptor tyrosine kinase (SU5416 and ZD6474; refs. 7, 8), and thyroid hormones (9) all play a major role in the metabolism of tumor cells by modifying the rate of oxygen consumption.

In the 1970s, arsenic trioxide (As_2O_3) was reported to induce complete remission in patients with acute promyelocytic leukemia (APL) in China (10). Additional studies confirmed that low doses of As_2O_3 could induce complete remission in 90% of relapsed APL patients (10). Importantly, it has become evident that the apoptotic effects of As_2O_3 are not restricted to APL cells but have also been observed in other malignant cells in preclinical studies, including myeloma cells, chronic myeloid leukemia cells, and various solid tumors cells, such as prostate, esophageal, and ovarian carcinomas (11–13).

Arsenic acts on cells through a variety of mechanisms, influencing numerous signal transduction pathways and resulting in a vast range of cellular effects that include apoptosis induction, growth inhibition, promotion, or inhibition of differentiation and inhibition of angiogenesis (11, 14–16). As_2O_3 also seems to inhibit mitochondrial respiratory function in human leukemia cells (17). We therefore hypothesized that As_2O_3 could be an important modulator of tumor oxygenation in solid tumors by affecting the oxygen consumption of tumor cells. The first step of the study was to monitor pO_2 in experimental tumors using electron paramagnetic resonance

Authors' Affiliations: [1]Biomedical Magnetic Resonance Group, [2]Laboratory of Pharmacokinetics, Metabolism, Nutrition and Toxicology, Louvain Research Institute; [3]Laboratory of Pharmacotherapy and [4]Center for Molecular Imaging and Experimental Radiotherapy, and [5]de Duve Institute, Université catholique de Louvain, Brussels, Belgium

Corresponding Author: Bernard Gallez, Louvain Drug Research Institute, Biomedical Magnetic Resonance Group, Laboratory of Pharmacokinetics, Metabolism, Nutrition and Toxicology, Avenue Mounier 73.40, B-1200, Université catholique de Louvain, Brussels, Belgium. Phone: 32-2-7647391; Fax: 32-2-764.73.90; E-mail: bernard.gallez@uclouvain.be

doi: 10.1158/0008-5472.CAN-11-1755

(EPR) oximetry (18) after administration of As_2O_3 to determine the window of increased tumor oxygenation. These results were confirmed by ^{19}fluorine MRI (^{19}F-MRI) oxygen mapping, a technique that can probe the spatial heterogeneity of response (19, 20). Patent blue staining (blood flow) and *in vitro* oxygen consumption experiments were done to investigate the origin of the observed increase in pO_2. The intracellular glutathione (GSH) content and the mitochondrial membrane potential were also evaluated to explain a possible mechanism by which As_2O_3 could decrease oxygen consumption. Finally, the window of increased oxygenation was exploited to enhance response of tumors to radiotherapy. Our study is the first report of the acute effect of As_2O_3 on oxygen consumption in solid tumors and provides a new rationale for combining As_2O_3 with radiotherapy.

Materials and Methods

Tumor model

Two tumor models were implanted by intramuscular injection in the rear leg of male mice: the transplantable mouse liver tumor (TLT) model in NMRI mice and the Lewis lung carcinoma (LLC) in C57Black6N mice. Measurements were done when the tumor size reached 8.0 ± 1.0 mm. All animal experiments were conducted in accordance with national animal care regulations.

Treatments

As_2O_3 was purchased from Sigma-Aldrich. For the treated group, As_2O_3 was dissolved in PBS (Invitrogen) and given by intraperitoneal injection (5 mg/kg body weight, 100 μL injected). Control animals were treated with PBS only. Animals were anesthetized by inhalation of isoflurane mixed with air in a continuous flow (3% induction, 1.8% maintain for a minimum of 15 minutes before any measurement).

Tumor oxygenation

Electron paramagnetic resonance oximetry. EPR oximetry, using charcoal (CX 0670-1; EM Sciences) as the oxygen-sensitive probe, was used to evaluate changes in tumor oxygenation after treatment with As_2O_3, using a protocol described previously (21). EPR spectra were recorded using an EPR spectrometer (Magnettech) with a low-frequency microwave bridge operating at 1.2 GHz and an extended loop resonator, or using a Bruker Elexsys system with an L-band microwave bridge working at 1.1 GHz and equipped with an E540R23 L-Band EPR coil resonator. A suspension of charcoal was slowly injected into the center of the tumor 1 day before measurement (100 mg/mL; 70 μL injected, particle size of 1–25 μm; needle diameter, 0.4 mm). The acute effect of As_2O_3 was measured by following the tumor pO_2 status before and for 2 hours after the single injection.

^{19}F-MRI measurements. MRI was done with a 4.7 T, 40-cm inner diameter bore system (Bruker Biospec) and a tunable ^{1}H/^{19}F surface coil. Parametric images of the spin-lattice relaxation time (T_1) were estimated using a snapshot inversion recovery (SNAP-IR) pulse sequence, using a protocol described previously (19). Hexafluorobenzene (HFB) was slowly injected into the tumor and deposited along 3 tracks (3 × 30 μL) encompassing central and peripheral regions. As_2O_3 was administered in 5 mice by a catheter and the tumor pO_2s were monitored for 2 hours. Two measurements were acquired as baseline before injection. The mice used for this study were different from those used for EPR oximetry.

Patent blue staining

Patent blue (Sigma-Aldrich) was used to obtain a rough estimate of the TLT tumor perfusion fraction 90 minutes after administration of As_2O_3 or PBS, using a protocol described previously (7, 8). The assay was applied on a separate cohort. Briefly, this technique involved the injection of 200 μL of Patent blue solution (1.25%) into the tail vein of the mice, which were sacrificed after 1 minute, with tumors excised and cut into 2 size-matched halves. For each with tumors, the percentage of stained area of the whole cross section was determined using an in-house program running on MatLab, used as an indicator of tumor perfusion fraction.

In vitro evaluation of oxygen consumption rate

TLT cells were cultured in Dulbecco's modified Eagle's medium (DMEM) containing 10% FBS, 4.5 mg/L glucose, and 1% penicillin–streptomycin. Confluent cells were suspended in medium without serum 2 hours before treatment with As_2O_3 (25 μmol/L) or PBS. EPR spectra were recorded on a Bruker EMX EPR spectrometer operating at 9 GHz. Tumor cells (2×10^7/mL) were suspended in 10% dextran in complete medium. A neutral nitroxide, ^{15}N 4-oxo-2,2,6,6-tetramethylpiperidine-d_{16}-^{15}N-1-oxyl, at 0.2 mmol/L (CDN Isotopes), was added to 100-μL aliquots of tumor cells that were then drawn into glass capillary tubes. Oxygen consumption rates were obtained by measuring the pO_2 in the closed tube over time and finding the slope of the resulting linear plot, using a protocol described previously (9).

Cell survival assay

Cellular viability was estimated by measuring the activity of lactate dehydrogenase (LDH), both in the culture medium and in the cell pellet obtained after centrifugation (22). The results were expressed as the ratio of released activity to total activity.

Tumor regrowth delay assay

The TLT tumor-bearing leg was irradiated locally with 10 Gy of 250 kV X-rays (RT 250; Philips Medical Systems; 1.2 Gy/min). The tumor was centered in a 3-cm circular irradiation field. A single-dose irradiation of 10 Gy was given 90 minutes after injection of As_2O_3 or PBS. After radiotherapy, tumor growth was determined daily using a caliper until the diameter reached 16 mm, at which time the mice were sacrificed. A linear fit was carried out between 8 and 16 mm, which allowed determination of the time to reach a particular size for each mouse.

Measurement of intracellular GSH

The glutathione content was determined using the Tietze enzyme recycling assay (23), with slight modifications (24). TLT cells were cultured in DMEM containing 10% FBS,

4.5 mg/L glucose, and 1% penicillin–streptomycin. Tumor cells were treated with As_2O_3 (25 μmol/L) or PBS over a period of 90 minutes for TLT cells. Cells were then washed twice with ice-cold PBS and then lysed with a solution of 5-sulfosalicylic acid (5%). After 2 freeze-thaw cycles, samples were centrifuged at 10,000 *g* for 10 minutes and the resulting supernatants were kept at −80°C. Ten microliters of the samples was then placed in a mixture containing 0.2 U/mL of glutathione reductase, 50 μg/mL 5,5′-dithio-bis(2-nitrobenzoic acid), and 1 mmol/L EDTA at pH 7. The reaction was initiated by the addition of 50 μmol/L NADPH, and changes in absorbance were recorded at 412 nm. GSH and oxidized glutathione were distinguished by the addition of methyl-2-vinylpyridine, and their respective concentrations were determined from appropriate standard curves. Results were normalized to the protein content using the method of Lowry and colleagues (25).

Measurement of mitochondrial membrane potential

TLT cells were treated with As_2O_3 (25 μmol/L) in 6-well plates. Mitochondrial membrane potential was monitored using a fluorescent cationic dye known as JC-1 (Sigma Mitochondria Staining Kit). In healthy cells, JC-1 enters the negatively charged mitochondria, where it aggregates and fluoresces red. In cells in which the mitochondrial potential has collapsed, JC-1 exists as monomers throughout the cell. When dispersed in this manner JC-1 fluoresces green. Consequently, mitochondrial depolarization is indicated by a decrease in the red–green fluorescence intensity ratio (26). Data acquisition was done using a FACSCalibur flow cytometer (Becton Dickinson), and data were analyzed with FlowJo software (Tree Star, Inc.). Valinomycin and carbonyl cyanide m-chlorophenylhydrazone (mCICCP) were used as positive controls (depolarizing agents).

Statistical analysis

Means ± SEs were compared using the unpaired Student *t* test or ANOVA (multiple comparisons post tests for 3 groups or more). *P* values less than 0.05 were considered statistically significant.

Results

As_2O_3 rapidly increases tumor oxygenation

The administration of As_2O_3 at 5 mg/kg induced an acute increase in pO_2 in TLT (Fig. 1A) and LLC (Fig. 1B) tumors, an effect that was not observed for the control group (Fig. 1A–B) or for the group treated at 1 mg/kg of As_2O_3 (data not shown). After injection of As_2O_3, the pO_2 increased rapidly in TLT and LLC tumors, after which pO_2 decreased, enabling a window of the increased oxygenation to be determined (Fig. 1). For TLT tumors, the mean tumor pO_2 (measured by EPR oximetry) after 90 minutes was 38.6 ± 7.2 mm Hg for treated mice ($n = 6$) and 4.3 ± 0.5 mm Hg for controls ($n = 6$; $P < 0.01$, *t* test). For LLC tumors, the mean pO_2 after 45 minutes was 10.5 ±1.3 mm Hg for treated mice ($n = 5$) and 4.3 ± 0.3 mm Hg for control mice ($n = 5$; $P < 0.01$, *t* test). The effect of 5 mg/kg of As_2O_3 on pO_2 was further confirmed by ^{19}F-MRI relaxometry in TLT tumors, which provides an estimation of the temporal and spatial heterogeneity of response. The mean tumor pO_2 was 15.9 ± 2.2 mm Hg before the injection of the drug and 30.8 ± 5.5 mm Hg 60 minutes after As_2O_3 injection (time of maximal pO_2, according to this oximetry technique; $P < 0.05$, *t* test, $n = 5$). The evolution of pO_2 over time, as measured by ^{19}F-MRI relaxometry, is shown in Fig. 2. ^{19}F-MRI relaxometry confirmed the trend of an early increase in pO_2 after As_2O_3 administration, although the treated and control dynamic curves were not significantly different due to a large variation in the pO_2 readings. Using ^{19}F-MRI relaxometry, it is possible to probe the spatial heterogeneity of response: color pO_2 maps and their corresponding histograms were generated, as shown in Fig. 3A. The color maps show an increase in pO_2 after treatment with As_2O_3, marked by a global increase in the red color (corresponding to pO_2 higher than 10 mm Hg). The histograms show a clear shift of the pO_2 values to the right after As_2O_3 treatment ($n = 5$; Fig. 3B). For all further experiments (flow estimation and therapeutic relevance), the experiments were conducted 90 minutes after injection of As_2O_3 in mice bearing the TLT tumor model.

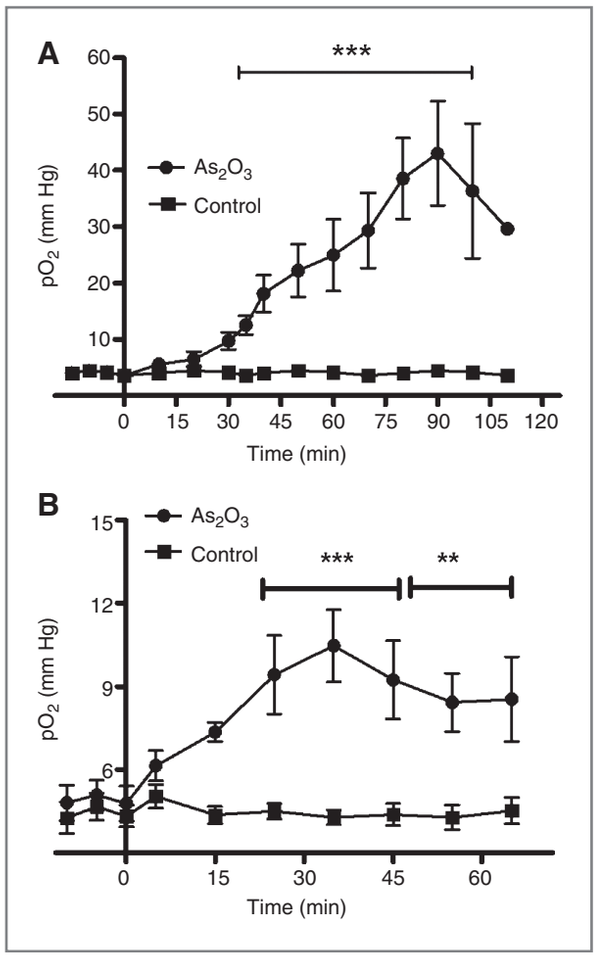

Figure 1. Tumor pO_2 measured by EPR oximetry in TLT (A, $n = 6$) and LLC (B, $n = 5$) tumors as a function of time (mean ± SE). As_2O_3 dose of 5 mg/kg was injected at time 0 after establishing a baseline. **, $P < 0.01$; ***, $P < 0.001$.

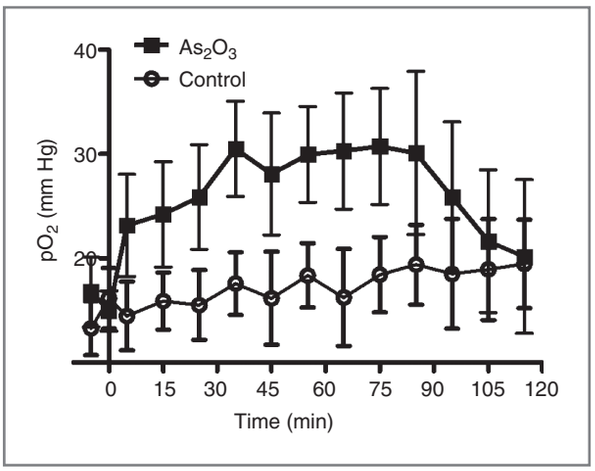

Figure 2. Tumor pO_2 measured by ^{19}F MRI in TLT tumors. As_2O_3 dose of 5 mg/kg has been injected at time 0 after establishing a baseline.

The reoxygenation induced by As_2O_3 is mediated by an effect on oxygen consumption

To explain the increase in pO_2 induced by As_2O_3, blood perfusion in TLT tumors was investigated using the Patent blue staining assay 90 minutes after As_2O_3 injection (Fig. 4A and B). This method has previously been validated by our group and compared with dynamic contrast-enhanced MRI data (6, 7). The colored area observed in tumors 1 minute after injection of the dye (Patent blue) was decreased in As_2O_3-treated mice ($n = 8$) compared with control mice ($n = 7$; 38.8 ± 4.6% vs. 61.2 ± 4.9%, $P < 0.01$, Fig. 4A), indicating that blood perfusion fraction

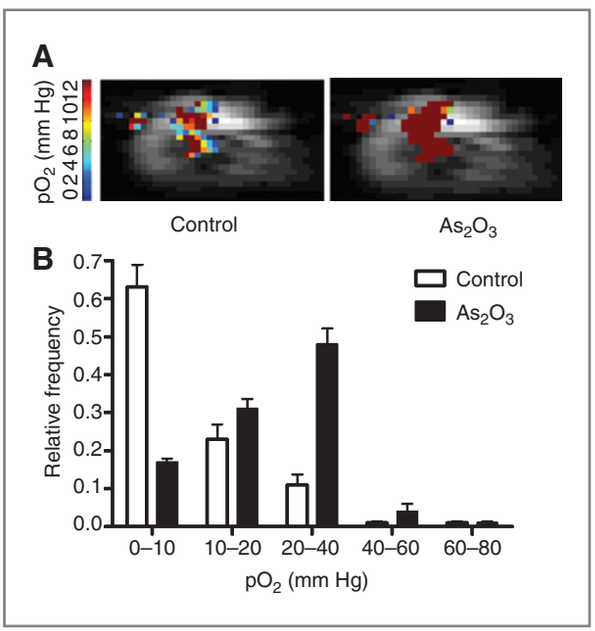

Figure 3. Typical oxygen maps of one TLT tumor before and after As_2O_3 treatment (A) and the corresponding histogram (B; mean ± SE, $n = 5$). The white and gray pixels correspond to the anatomic image of the tumor and color pixels to the pO_2 measurements based on the distribution of the HFB in the tumor.

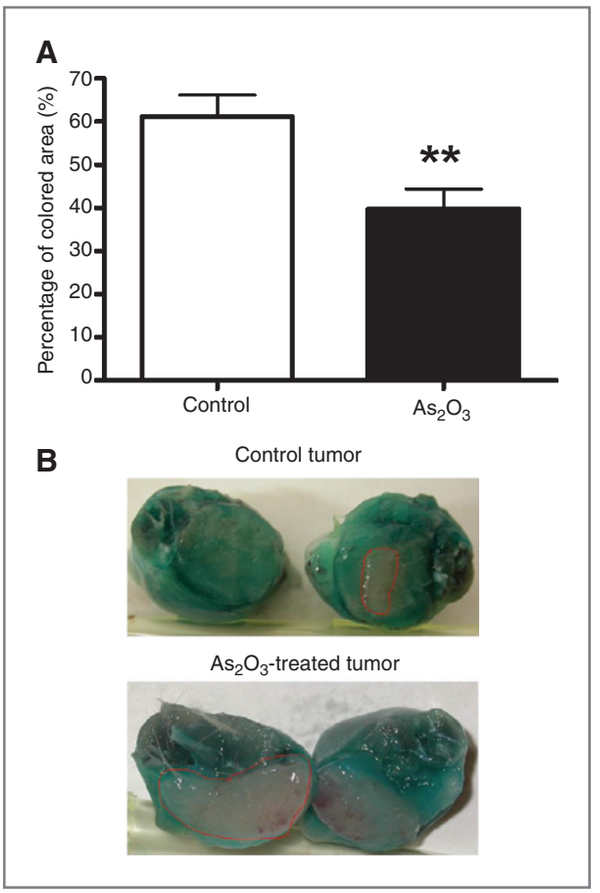

Figure 4. Effect of As_2O_3 on blood perfusion measured by patent blue staining. A, percentage of coloration and perfusion decrease in treated mice ($n = 8$) compared with control mice ($n = 7$). **, $P < 0.01$. B, typical image of tumor sections showing typical staining in control and treated tumor. The staining was lower in treated mice. Perfusion measurements were done 90 minutes after As_2O_3 injection (5 mg/kg). The red lines are drawn to define regions of interest on nonperfused areas, as described in Materials and Methods.

was decreased in treated mice. Typical images are shown in Fig. 4B.

The oxygen consumption was investigated *in vitro* on TLT tumor cells exposed to As_2O_3 during 90 minutes. The incubation in the presence of As_2O_3 significantly decreased the rate of oxygen consumption (Fig. 5), with mean slopes of −1.68 ± 0.07 μmol/L/min ($n = 6$) and −3.5 ± 0.1 μmol/L/min ($n = 7$; $P < 0.001$) for treated and control cells, respectively. As_2O_3-treated cells thus consumed oxygen 2 times slower than control cells. To exclude a possible direct cytotoxic effect of As_2O_3, we also measured the activity of LDH in TLT cells 90 minutes and 4 hours after incubation in the presence of As_2O_3. Treatment induced LDH leakage of 23.4 ± 2.5% (90 minutes after treatment) and 27 ± 2.1% (4 hours after treatment) compared with 34.1 ± 2.1% and 34.2 ± 2.3% (similar timings) in control mice. These results indicated that this concentration of As_2O_3 (25 μmol/L) did not influence the viability of TLT cells early after the exposure (1-way ANOVA).

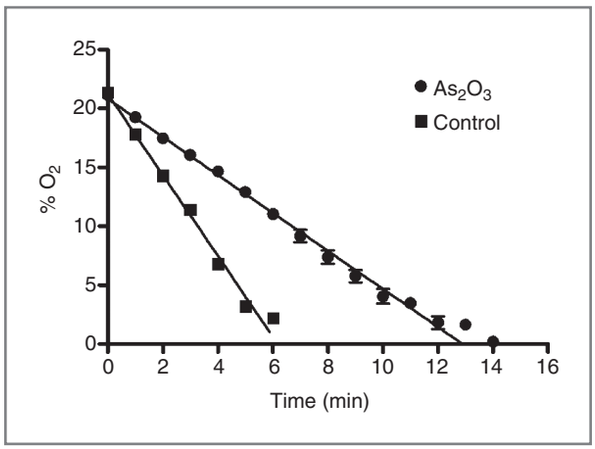

Figure 5. Effect of As_2O_3 administration on tumor oxygen consumption rate in TLT tumor cells. Oxygen consumption measurements were done 90 minutes after As_2O_3 treatment (25 μmol/L). As_2O_3-pretreated cells consumed oxygen significantly more slowly than control cells ($n = 6$ for treated cells and $n = 7$ for control cells).

To determine whether the lowering of intracellular GSH content was a possible mechanism by which As_2O_3 could decrease the oxygen consumption of tumor cells, we measured the intracellular content of GSH. GSH contents were 18.3 nmol/mg protein and 42.6 nmol/mg protein for TLT-treated and control cells, respectively (Fig. 6A). Inhibiting GSH production may lead to oxidative stress by enhancing intracellular reactive oxygen species (ROS), and accumulation of intracellular ROS leads to disruption of the mitochondrial membrane potential. This hypothesis is supported by the fact that the number of TLT cells with depolarized mitochondria was increased in the presence of As_2O_3 as shown in the JC-1 assay (Fig. 6B).

As_2O_3 radiosensitizes tumors by an oxygen effect

To evaluate the effect of As_2O_3 on tumor regrowth after irradiation, tumor-bearing mice were irradiated with a single dose of 10 Gy of X-rays. Figure 7A shows the tumor growth of TLT tumors treated or not with As_2O_3, with or without irradiation. In the nonirradiated groups, there was no significant difference between tumors treated with PBS and those treated with As_2O_3 ($P > 0.05$). All irradiated groups showed a significant regrowth delay compared with their respective control group ($P < 0.01$). When irradiation was applied during the time window of increased oxygenation produced by As_2O_3 administration, the regrowth delay (33.2 ± 2 days to reach 12 mm) was significantly increased compared with irradiation alone (14.8 ± 2.4 days; $P < 0.001$, 1-way ANOVA, Tukey multiple comparison test, Fig. 7B), resulting in a 2.2-fold increase in radiation response. Importantly, tumors were individually monitored with EPR oximetry after administration of As_2O_3 to make sure that the pO_2 was increased at the time of irradiation. To discriminate between an oxygen effect and a direct radiosensitizing effect, we also irradiated a group of As_2O_3-treated mice whose legs had been temporarily ligated to induce complete hypoxia at the time of irradiation. We

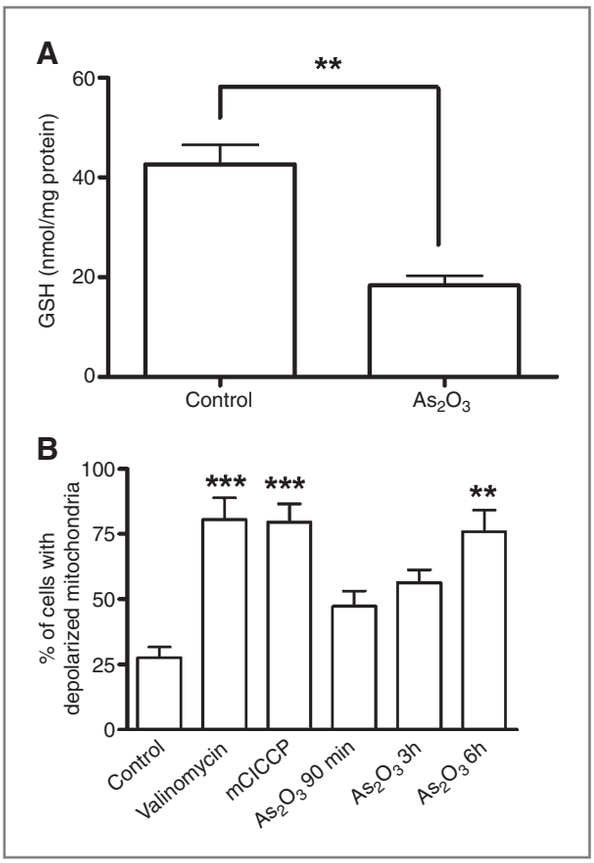

Figure 6. A, Intracellular GSH level in TLT tumor cells. GSH levels were measured 90 minutes after As_2O_3 treatment (25 μmol/L). The GSH levels decrease in As_2O_3-treated cells compared with control cells. GSH levels were expressed as nmol/mg protein. GSH values are the mean of triplicate measurements. **, $P < 0.01$; ***, $P < 0.001$. B, % of TLT cells with depolarized mitochondria as measured by the JC-1 assay. Effect of incubation in the presence of As_2O_3 (25 μmol/L) compared with untreated cells. Valinomycin and mCICCP were used as positive controls.

checked the efficiency of the ligation by measuring pO_2 using EPR oximetry: In these conditions, the tumors were anoxic [$pO_2 = 0.1 \pm 0.2$ mm Hg ($n = 3$) after leg ligation]. The regrowth delays were similar for the control irradiated group and the As_2O_3 + hypoxia irradiated group (Fig. 7B). Finally, in an independent set of mice that were not treated with As_2O_3, we found no significant difference in regrowth delays between an irradiated group and a similar group that was deprived with oxygen at the time of irradiation (by leg ligation; 12 ± 0.6 days vs. 11.1 ± 0.9 days), indicating that this tumor model presents a highly hypoxic pattern that is relevant to study hypoxia-induced radioresistance. As_2O_3 therefore induces an additional regrowth delay due to an oxygen effect. In Fig. 7C, we used Kaplan–Meier curves to compare survival times (times at which mice were sacrificed, when the tumor diameter reached 16 mm) in the different groups. As_2O_3 administration combined with radiation extended the median survival of mice by more than 20 days compared with control.

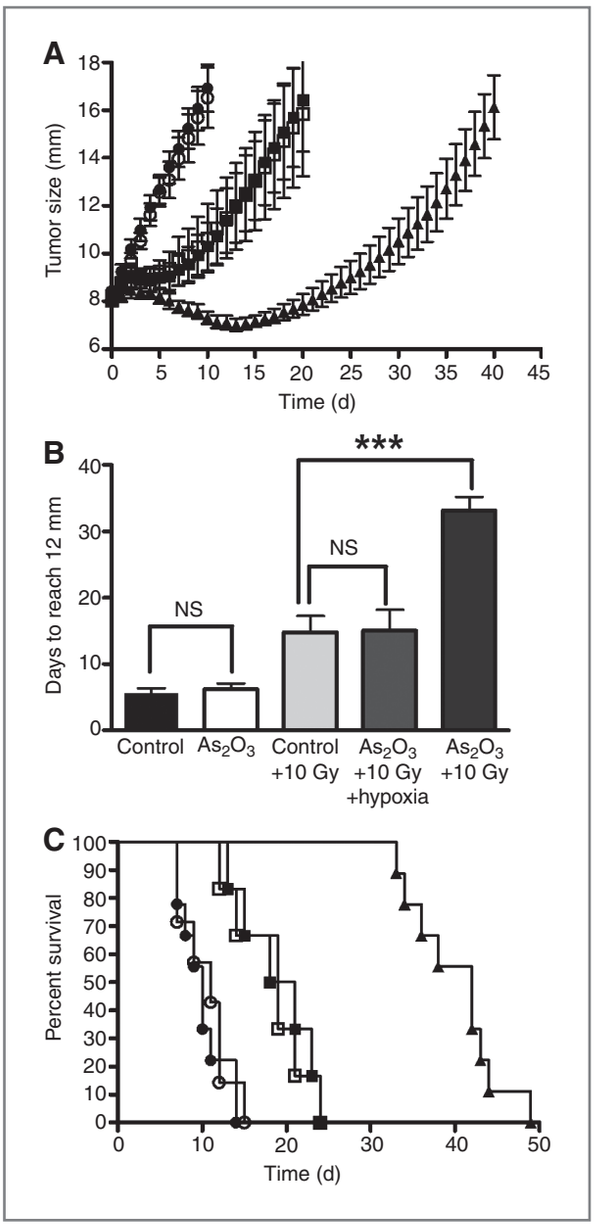

Figure 7. A, effect of As_2O_3 on TLT tumor regrowth. Mice were treated with PBS (●, $n = 9$), As_2O_3 (○, $n = 7$), 10 Gy of radiotherapy 90 minutes after PBS (■, $n = 6$), 10 Gy of radiotherapy 90 minutes after As_2O_3 (▲, $n = 9$), or 10 Gy of radiotherapy 90 minutes after As_2O_3 plus tumor ligation at the time of irradiation (□, $n = 6$). Each point represents the mean tumor size ± SE. B, time to reach 12 mm (days). Results are mean ± SE, 1-way ANOVA Tukey multiple comparison test. ***, $P < 0.001$. C, Kaplan–Meier analysis of survival. Survival curve (times when the tumor diameter reached 16 mm) for each group.

Discussion

The major findings of this study are (i) As_2O_3 significantly reduced the tumor hypoxic fraction ($pO_2 < 10$ mm Hg) early after administration of a single dose; (ii) the early increased oxygenation effect was linked to a decrease in tumor cell oxygen consumption rate; (iii) As_2O_3 significantly increased the effectiveness of tumor radiotherapy when irradiation was performed in the time window of increased oxygenation.

In this study, we report that As_2O_3 can induce an acute and transient increase in tumor oxygenation in experimental tumors. The basal pO_2 values and the time window of the increased oxygenation in TLT tumors measured using EPR and ^{19}F-MRI relaxometry techniques were not exactly the same. The differences in observed pO_2 readings coming from these techniques can be partly explained by different factors that have been discussed in detail in other methodologic publications, including differences in sampling volumes (18–20, 27). The fact that we used 2 independent sets of tumor-bearing mice may also explain some differences observed. Despite differences in the nature of the measurements, both techniques indicated that the increase in oxygenation was rapidly occurring after As_2O_3 administration, that it lasted for more than 1 hour, and that this effect was distributed in all areas of the tumors. A previous study reported an increase in pO_2, measured with an Eppendorf pO_2 histograph, after chronic administration of As_2O_3 in FSa II tumors; the maximal increased oxygenation was observed at day 3 (28). The authors interpreted the As_2O_3-induced increase in tumor oxygenation to be related to an increased supply of oxygen to the remaining viable regions of the tumor and a decrease in total oxygen demand of the tumor because of the significant amount of cell death involved in As_2O_3-induced necrosis (28). As the increased tumor oxygenation may result from an increase in oxygenation delivery and/or a decrease in oxygen consumption, we investigated both aspects to determine the origin of the observed effect responsible for the rapid change in tumor oxygenation. We showed a decrease in tumor perfusion after administration of As_2O_3, which excludes this parameter as a possible cause of the early tumor reoxygenation. This is in accordance with other studies that showed that a single dose of As_2O_3 induced a decrease in perfusion in tumors (28, 29, 30). Tumor cell oxygen consumption was reduced significantly after exposure to As_2O_3. We excluded a possible direct cytotoxic effect of As_2O_3 by measuring the activity of LDH in TLT cells after As_2O_3 exposure. LDH assay is a well-recognized test used to assess plasma membrane breakdown as a sign of cytotoxicity. We excluded the MTT assay because it is dependent on the mitochondrial function and a clonogenic assay because the effect of As_2O_3 was rapid and transient. Our results indicate that the concentration of As_2O_3 used in this assay (25 μmol/L) did not influence the viability of TLT cells early after the exposure. A mathematical model predicted that modification of oxygen consumption would be much more efficient at alleviating hypoxia than modification of oxygen delivery (2), a theoretical hypothesis that has been extensively shown experimentally by our group (4–9). Thus, it is theoretically and experimentally possible for tumor oxygenation to improve even in the face of diminished perfusion (31). In comparison with previously described approaches to target oxygen consumption in TLT tumors (32), As_2O_3 induces a higher increase in oxygenation than all previously considered inhibitors. Also, the resulting factor of increase in tumor regrowth delay is

above 2, which is superior to the effect observed with the majority of consumption inhibitors.

The effects of As_2O_3 on oxygen consumption have already been observed *in vitro* by others, and the suggested mechanism was the inhibition of respiration upstream of complex IV in the mitochondrial respiratory chain (17). Another mechanism could involve the redox status of the tumor. The GSH redox system is known to modulate the effects of As_2O_3. Previous findings showed that sensitivity to As_2O_3-induced apoptosis was inversely related to the intracellular GSH content and that pharmacologic modulation of intracellular GSH content altered sensitivity to As_2O_3 (33). A study also showed that As_2O_3-induced adhesion molecule expression *in vitro* was abolished when the antioxidant *N*-acetyl-cysteine (NAC) was introduced prior to exposure, whereas the addition of NAC *in vivo* partially blocked As_2O_3-induced vascular shutdown (30). In our study, we observed a decrease in GSH content in As_2O_3-treated cells compared with control cells. This decrease in GSH levels could explain the inhibitory effect of As_2O_3 on oxygen consumption. Indeed, the GSH redox system represents one of the most important cellular defense systems against oxidative stress. Inhibiting GSH production may lead to oxidative stress by enhancing intracellular ROS, and accumulation of intracellular ROS leads to disruption of the mitochondrial membrane potential (34). This hypothesis is supported by the fact that the number of TLT cells with depolarized mitochondria was increased after exposure to As_2O_3. It is important to note that changes in oxygen consumption can occur a long time before changes in membrane potential become measurable (26). Overall, these observations indicate that As_2O_3 could act on the mitochondrial respiratory chain by enhancing intracellular ROS production mediated by decreased GSH levels. Although these experiments provide rational mechanisms that may explain the change in oxygen consumption by the tumor cells and increase in tumor oxygenation, it is important to note that it is difficult to extrapolate the kinetics of the effects observed *in vivo* from these *in vitro* experiments, as the result will be dependent on the dynamic evolution in concentration of As_2O_3 (perfusion and washout) inside the solid tumor.

We conducted radiosensitizing experiments to test the therapeutic value of the use of As_2O_3 in combination with radiotherapy. There was a significant increase in the response of tumors to radiotherapy (by a factor of 2.2) when X-ray irradiation was applied during the increased oxygenation window. As_2O_3 has previously been shown to induce tumor growth delay and to improve fractionated radiotherapy response in other studies that considered different mechanisms and timings of administration (28, 29, 35, 36). Lew and colleagues showed a significant regrowth delay after a single dose or fractionated schedule of radiation when As_2O_3 was administered 60 minutes after radiation, explained by the increased production of TNF-α, known to enhance the antitumor effects of radiation (29). In other tumor cell lines, it seemed that As_2O_3 was also able to directly radiosensitize tumor cells, contrary to our findings in TLT cells (36). One area related to As_2O_3 exposure that has been widely studied is the depletion of the GSH level in cells, which may lead to oxidative stress and has been linked to increases in radiosensitivity (36, 37). Griffin and colleagues reported the greatest regrowth delay when combining treatment and radiation every 3 days, at the time of maximal tumor oxygenation in their model, suggesting that the oxygen level is an important factor in terms of radiosensitization by As_2O_3 (28). In these chronic experiments, the main factor was likely the decrease in oxygen demand due to the cell death. In this study, the acute increased oxygenation after administration of a single dose of As_2O_3 was likely due to an effect on the mitochondrial respiration. Furthermore, tumors that were clamped during the irradiation were not radiosensitized, which identifies the "oxygen effect" as the major factor responsible for the rapid radiosensitization of TLT tumors by As_2O_3, rather than an intrinsic direct radiosensitizing effect of the drug.

It is important to mention that there are large differences between the dose used in humans and animals. The usual dose used to treat APL is 0.15 mg/kg/d, and larger doses (up to 35 mg/kg/d) have been used in phase II clinical trials in patients with metastatic melanoma and renal cell carcinoma (38–40). In mice and rats, the usual doses ranged from 2 to 8 mg/kg (28, 30) and generally exceed the doses used in humans. This is related to the difference in route of administration [i.v. vs. intraperitoneal (i.p.)] and the good tolerance of mice to As_2O_3 (the LD_{50} in mice is 11–11.8 mg/kg i.p), which is linked to a difference in metabolism. The metabolism of arsenic in humans produces more toxic methylated arsenic compounds than in other animals (41). Even at a high dose (6.5 mg/kg), the levels of As_2O_3 in brain, kidney, and liver were low and the histologic examination showed no pathologic changes (42). No obvious sign of toxicity was observed in studies that investigated the possible adverse effects of combined treatment with As_2O_3 and radiation (43, 44). More information about arsenic toxicity and pharmacokinetics is available in the official document linked to the Initial Marketing Authorization of Trisenox (45). Finally, it has also been shown that As_2O_3 selectively accumulated in tumors (28, 29, 41). As the difference in dose is approximately a 10-fold increased sensitivity to arsenic effects in humans and as the extrapolation of the animal data to humans is not straightforward, initial clinical studies that could benefit from our present observations should likely start with doses currently used in the clinic to treat APL or solid tumors.

In conclusion, we report for the first time that a single dose of As_2O_3 can decrease oxygen consumption by tumor cells in experimental tumors, resulting in a transient increased oxygenation of the tumors. This increased oxygenation window could be exploited to significantly enhance tumor radiation response, after individual monitoring of the tumor pO_2 before radiotherapy. The oxygen effect was identified as the major factor involved in the sensitization process induced by As_2O_3. Although additional fractionated radiation studies and TCD_{50} experiments should be conducted for further preclinical validation in a larger panel of tumor models, our study suggests that As_2O_3 could be used as a potential cotreatment for radiation therapy when this is applied at the time of maximum increased oxygenation induced by the drug.

Disclosure of Potential Conflicts of Interest

No potential conflicts of interest were disclosed.

Acknowledgments

This work is supported by grants from the Belgian National Fund for Scientific Research (FNRS), the Televie, the Fonds Joseph Maisin, the Saint-Luc Foundation, the "Actions de Recherches Concertées-Communauté Française de Belgique-ARC 09/14-020", and the "Pôle d'attraction Interuniversitaire PAI VI (P6/38)". B.F. Jordan is a research associate of the FNRS.

The costs of publication of this article were defrayed in part by the payment of page charges. This article must therefore be hereby marked *advertisement* in accordance with 18 U.S.C. Section 1734 solely to indicate this fact.

Received May 31, 2011; revised November 25, 2011; accepted November 29, 2011; published OnlineFirst December 2, 2011.

References

1. Tatum JL, Kelloff GJ, Gillies RJ, Arbeit JM, Brown JM, Chao KS, et al. Hypoxia: importance in tumor biology, noninvasive measurement by imaging, and value of its measurement in the management of cancer therapy. Int J Radiat Biol 2006;82:699–757.
2. Secomb TW, Hsu R, Ong ET, Gross JF, Dewhirst MW. Analysis of the effects of oxygen supply and demand on hypoxic fraction in tumors. Acta Oncol 1995;34:313–6.
3. Biaglow JE, Manevich Y, Leeper D, Chance B, Dewhirst MW, Jenkins WT, et al. MIBG inhibits respiration: potential for radio- and hyperthermic sensitization. Int J Radiat Oncol Biol Phys 1998; 42:871–6.
4. Jordan BF, Gregoire V, Demeure RJ, Sonveaux P, Feron O, O'Hara J, et al. Insulin increases the sensitivity of tumors to irradiation: involvement of an increase in tumor oxygenation mediated by a nitric oxide-dependent decrease of the tumor cells oxygen consumption. Cancer Res 2002;62:3555–61.
5. Crokart N, Radermacher K, Jordan BF, Baudelet C, Cron GO, Grégoire V, et al. Tumor radiosensitization by antiinflammatory drugs: evidence for a new mechanism involving the oxygen effect. Cancer Res 2005;65:7911–6.
6. Crokart N, Jordan BF, Baudelet C, Cron GO, Hotton J, Radermacher K, et al. Glucocorticoids modulate tumor radiation response through a decrease in tumor oxygen consumption. Clin Cancer Res 2007;13: 630–5.
7. Ansiaux R, Baudelet C, Jordan BF, Crokart N, Martinive P, DeWever J, et al. Mechanism of reoxygenation after antiangiogenic therapy using SU5416 and its importance for guiding combined antitumor therapy. Cancer Res 2006;66:9698–704.
8. Ansiaux R, Dewever J, Gregoire V, Feron O, Jordan BF, Gallez B. Decrease in tumor cell oxygen consumption after treatment with vandetanib (ZACTIMA; ZD6474) and its effect on response to radiotherapy. Radiat Res 2009;172:584–91.
9. Jordan BF, Christian N, Crokart N, Gregoire V, Feron O, Gallez B. Thyroid status is a key modulator of tumor oxygenation: implication for radiation therapy. Radiat Res 2007;168:428–32.
10. Zhu J, Chen Z, Lallemand-Breitenbach V, de Thé H. How acute promyelocytic leukaemia revived arsenic. Nat Rev Cancer 2002;2: 705–13.
11. Maeda H, Hori S, Nishitoh H, Ichijo H, Ogawa O, Kakehi Y, et al. Tumor growth inhibition by arsenic trioxide (As2O3) in the orthotopic metastasis model of androgen-independent prostate cancer. Cancer Res 2001;61:5432–40.
12. Shen ZY, Zhang Y, Chen JY, Chen MH, Shen J, Luo WH, et al. Intratumoral injection of arsenic to enhance antitumor efficacy in human esophageal carcinoma cell xenografts. Oncol Rep 2004;11: 155–9.
13. Bornstein J, Sagi S, Haj A, Harroch J, Fares F. Arsenic trioxide inhibits the growth of human ovarian carcinoma cell line. Gynecol Oncol 2005;99:726–9.
14. Woo SH, Park IC, Park MJ, Lee HC, Lee SJ, Chun YJ, et al. Arsenic trioxide induces apoptosis through a reactive oxygen species-dependent pathway and loss of mitochondrial membrane potential in HeLa cells. Int J Oncol 2002;21:57–63.
15. Miller WH Jr, Schipper HM, Lee JS, Singer J, Waxman S. Mechanisms of action of arsenic trioxide. Cancer Res 2002;62:3893–903.
16. Xiao YF, Liu SX, Wu DD, Chen X, Ren LF. Inhibitory effect of arsenic trioxide on angiogenesis and expression of vascular endothelial growth factor in gastric cancer. World J Gastroenterol 2006;12: 5780–6.
17. Pelicano H, Feng L, Zhou Y, Carew JS, Hileman EO, Plunkett W, et al. Inhibition of mitochondrial respiration: a novel strategy to enhance drug-induced apoptosis in human leukemia cells by a reactive oxygen species-mediated mechanism. J Biol Chem 2003;278:37832–9.
18. Gallez B, Baudelet C, Jordan BF. Assessment of tumor oxygenation by electron paramagnetic resonance: principles and applications. NMR Biomed 2004;17:240–62.
19. Jordan BF, Cron GO, Gallez B. Rapid monitoring of oxygenation by 19F magnetic resonance imaging: Simultaneous comparison with fluorescence quenching. Magn Reson Med 2009;61:634–8.
20. Zhao D, Jiang L, Mason RP. Measuring changes in tumor oxygenation. Methods Enzymol 2004;386:378–418.
21. Gallez B, Jordan BF, Baudelet C, Misson PD. Pharmacological modifications of the partial pressure of oxygen in murine tumors: evaluation using *in vivo* EPR oximetry. Magn Reson Med 1999;42: 627–30.
22. Galluzzi L, Aaronson SA, Abrams J, Alnemri ES, Andrews DW, Baehrecke RH, et al. Guidelines for the use and interpretation of assays for monitoring cell death in higher eukaryotes. Cell Death Differ 2009;16: 1093–107.
23. Tietze F. Enzymic method for quantitative determination of nanogram amounts of total and oxidized glutathione: applications to mammalian blood and other tissues. Anal Biochem 1969;27:502–22.
24. Griffith OW. Determination of glutathione and glutathione disulfide using glutathione reductase and 2-vinylpyridine. Anal Biochem 1980;106:207–12.
25. Lowry OH, Rosebrough NJ, Farr AL, Randall RJ. Protein measurement with the Folin phenol reagent. J Biol Chem 1951;193:265–75.
26. Cottet-Rousselle C, Ronot X, Leverve X, Mayol JF. Cytometric assessment of mitochondria using fluorescent probes. Cytom Part A 2011;79:405–25.
27. Robinson SP, Griffiths JR. Current issues in the utility of 19F nuclear magnetic resonance methodologies for the assessment of tumour hypoxia. Philos Trans R Soc Lond B Biol Sci 2004;359: 987–96.
28. Griffin RJ, Williams BW, Park HJ, Song CW. Preferential action of arsenic trioxide in solid-tumor microenvironment enhances radiation therapy. Int J Radiat Oncol Biol Phys 2005;61:1516–22.
29. Lew YS, Kolozsvary A, Brown SL, Kim JH. Synergistic interaction with arsenic trioxide and fractionated radiation in locally advanced murine tumor. Cancer Res 2002;62:4202–5.
30. Griffin RJ, Monzen H, Williams BW, Park H, Lee SH, Song CW. Arsenic trioxide induces selective tumour vascular damage via oxidative stress and increases thermosensitivity of tumours. Int J Hyperthermia 2003;19:575–89.
31. Dewhirst MW, Cardenas Navia I, Brizel DM, Willett C, Secomb TW. Multiple etiologies of tumor hypoxia require multifaceted solutions. Clin Cancer Res 2007;13:375–7.
32. Jordan BF, Gallez B. Surrogate MR markers of response to chemo- or radiotherapy in association with co-treatments: a retrospective analysis of multi-modal studies. Contrast Media Mol Imag 2010;5: 323–32.
33. Dai J, Weinberg RS, Waxman S, Jing Y. Malignant cells can be sensitized to undergo growth inhibition and apoptosis by arsenic

trioxide through modulation of the glutathione redox system. Blood 1999;93:268–77.
34. Dalton WS. Targeting the mitochondria: an exciting new approach to myeloma therapy. Clin Cancer Res 2002;8:3643–5.
35. Kim JH, Lew YS, Kolozsvary A, Ryu S, Brown SL. Arsenic trioxide enhances radiation response of 9L glioma in the rat brain. Radiat Res 2003;160:662–6.
36. Monzen H, Griffin RJ, Williams BW, Amano M, Ando S, Hasegawa T. Study of arsenic trioxide-induced vascular shutdown and enhancement with radiation in solid tumor. Radiat Med 2004;22:205–11.
37. Jones EL, Douple EB. The effect of *in vivo* GSH depletion on thermosensitivity, radiosensitivity and thermal radiosensitization. Int J Hyperthermia 1990;6:951–5.
38. Vuky J, Yu R, Schwartz L, Motzer RJ. Phase II clinical in patients with metastatic renal cell carcinoma. Invest New Drugs 2002;20: 327–30.
39. Kim KB, Bedikian AY, Camacho LH, Papadopoulos NE, McCullough C. A phase II trial of arsenic trioxide in patients with metastatic melanoma. Cancer 2005;104:1687–92.
40. Tarhini AA, Kirkwood JM, Tawbi H, Gooding WE, Islam MF, Agarwala SS. Safety and efficacy of arsenic trioxide for patients with advanced metastatic melanoma. Cancer 2008;112:1131–8.
41. Carter DE, Aposhian HV, Gandolfi AJ. The metabolism of inorganic oxides, gallium arsenide, and arsine: a toxicological review. Toxicol Appl Pharmacol 2003;193:309–34.
42. Kito M, Matsumoto K, Wada N, Sera K, Futatsugawa S, Naoe T, et al. Antitumor effect of arsenic trioxide in murine xenograft model. Cancer Sci 2003;94:1010–4.
43. Ning S, Knox SJ. Optimization of combination therapy of arsenic trioxide and fractionated radiotherapy for malignant glioma. Int J Radiat Oncol Biol Phys 2006;65:493–8.
44. Xie LX, Lin XH, Li DR, Chen JY, Hong CQ, Du CW. Synergistic therapeutic effect of arsenic trioxide and radiotherapy in BALB/C nude mice bearing nasopharyngeal carcinoma xenografts. Exp Oncol 2007;29:45–8.
45. The Official document linked to the Initial Marketing Authorization of Trisenox (European Public Assessment Report - Scientific Discussion - 28/10/2005). Available from: http://www.ema.europa.eu/.